1993

# The Soliton Transform and a Possible Application to Nonlinear Alfvén Waves in Space

T Hada
*Kyushu University*

Robert L. Hamilton
*George Fox University*, rhamilto@georgefox.edu

C F. Kennel
*University of California - Los Angeles*

GEOPHYSICAL RESEARCH LETTERS, VOL. 20, NO. 9, PAGES 779-782, MAY 5, 1993

# THE SOLITON TRANSFORM AND A POSSIBLE APPLICATION TO NONLINEAR ALFVÉN WAVES IN SPACE

T. Hada

Department of Physics, College of General Education, Kyushu University

R. L. Hamilton

Program in Applied Mathematics, University of Arizona

C. F. Kennel

Department of Physics, University of California at Los Angeles

*Abstract:* We apply the inverse scattering transform (IST) based upon the Derivative Nonlinear Schrödinger (DNLS) equation to a complex time series of nonlinear Alfvén wave data generated by numerical simulation. The IST describes the long-time evolution of quasi-parallel Alfvén waves more efficiently than the Fourier transform, which is adapted to linear, not nonlinear, problems. When we add dissipation, so the conditions for the validity of the DNLS are not strictly satisfied, the IST continues to provide a compact description of the wave-field in terms of a small number of decaying envelope solitons. Since large amplitude Alfvén waves and other nonlinear waves play essential roles in various space environments—the solar wind is one obvious example—we suggest that it may be of interest to investigate how inverse scattering transforms can be developed into practical tools for the analysis of space data.

## Introduction

It may be possible to create a data-adapted and physics-adapted transform that is more efficient than the Fourier transform for the analysis of nonlinear waves in space. The transform is based on the well-established Inverse Scattering Method for solving weakly nonlinear dispersive wave equations. We apply the method to the Derivative Nonlinear Schrödinger (DNLS) Equation, perhaps the richest equation for which it has been elaborated.

The DNLS describes finite amplitude Alfvén waves, which have been found in the solar wind (Burlaga, 1983), near planetary bow shocks (Greenstadt *et al.*, 1968; Hoppe *et al.*, 1981, 1982; Smith *et al.*, 1983), interplanetary shocks (Kennel *et al.*, 1984a,b) and comets (Scarf *et al.*, 1986; Tsurutani and Smith, 1986a,b). A variety of energy sources are known to generate Alfvén waves to amplitudes where nonlinearity can modify the waveform (c.f., Sentman *et al.*, 1981). The observed waveforms range from almost monochromatic circularly polarized waves to steepened compressional waves whose complex envelopes clearly suggest nonlinear wave evolution. Other prominent features include discrete wave packets, mixed polarization, linear polarization, and rapid phase and polarization changes (Hoppe *et al.*, 1981; Tsurutani *et al.*, 1990a,b). Few of these features are efficiently described by the Fourier transform, but many of them turn up in various solutions of the DNLS, so a DNLS-based transform might be of interest.



Paper number 93GL00073
0094-8534/93/93GL-00073$03.00

## The Derivative Nonlinear Schrödinger Equation (DNLS) and Its Inverse Scattering Transform (IST)

By applying a quasi-static approximation in which hydrodynamic nonlinearities and steepening are weak, Rogister (1971) derived a kinetic equation describing the long time evolution of the Alfvén waves. Essentially the same equation was subsequently obtained using two-fluid theory (Mjølhus, 1974; Mio *et al.*, 1976; Spangler and Sheerin, 1982). The fluid version, now known as the Derivative Nonlinear Schrödinger Equation (DNLS), reads

$$\frac{\partial b}{\partial t} + \alpha\frac{\partial}{\partial x}(|b|^2 b) + i\delta\frac{\partial^2 b}{\partial x^2} = 0 \ , \tag{1}$$

where x is the direction of propagation and the background magnetic field, $b=(B_y+iB_z)/B_x$ is the complex, transverse wave magnetic field normalized to $B_x$(=const); $\alpha/C_A=C_i^2/4(C_i^2-C_s^2)$, where $C_A$, $C_i$, $C_s$ are the Alfvén, intermediate, and sound speeds, respectively; and $2\delta/C_A=c/\omega_{pi}$ is the ion inertia dispersion length.

The DNLS describes the nonlinear coupling between weakly nonlinear, weakly dispersive, quasi-parallel, "shear Alfvén waves" and "magnetosonic" waves, which have almost the same phase and group speeds. Its oblique limits match the Korteweg-de Vries (KdV) description of the magnetosonic wave and the modified Korteweg-de Vries (mKdV) description of the Alfvén wave; for large wave numbers, it reduces to the nonlinear Schrödinger description of the left-hand (LH) and right-hand (RH) cyclotron modes (Kennel *et al.*, 1988).

Many nonlinear dispersive equations can be solved using essentially linear techniques. The simplest such equation, the KdV, is completely solved by mapping the nonlinear KdV equation into the linear Schrödinger equation, solving the associated scattering problem, and inverting. Two points are important to us here. First, just as Fourier harmonics characterize linear system, a localized nonlinear entity, the soliton, characterizes the KdV system. A wave envelope that seems complex to the Fourier transform may be a superposition of just a few solitons. Secondly, the measured wave profile determines the types of solitons in the transform, which is thus automatically data-adapted. We call this the Inverse Scattering Transform (IST), or soliton transform.

Next we describe the DNLS-IST for "vanishing boundary conditions", in which b approaches 0 as $x \to \pm\infty$ (Kaup and Newell, 1978). The DNLS is also integrable under several other types of boundary conditions (Kawata and Inoue, 1978; Kawata *et al.*, 1980; Prikarpatskii, 1981). Hereafter we let $\alpha=\delta=1$ in (1) by scale transformations, $t \to \delta t/\alpha^2$ and $x \to \delta x/\alpha$. We find b(x,t) for any t>0, given initial magnetic field data, b(x,t=0), by considering the related scattering problem for the complex vector function $\Psi(\lambda,x,t)$,

$$\frac{\partial \Psi}{\partial x} = D(\lambda,x,t)\Psi, \qquad D = i\lambda \begin{bmatrix} -\lambda & -ib \\ -ib^* & \lambda \end{bmatrix}, \tag{2}$$

where $\lambda$ is a complex eigenvalue and an asterisk denotes complex conjugate. Since $b \to 0$ as $x \to \pm\infty$, an asymptotic form of $\Psi$ can be written as

$$\Psi \sim \begin{bmatrix} e^{-i\lambda^2 x} \\ 0 \end{bmatrix} \text{ as } x \to -\infty \ ; \ \Psi \sim \begin{bmatrix} s_{11} e^{-i\lambda^2 x} \\ s_{21} e^{i\lambda^2 x} \end{bmatrix} \text{ as } x \to \infty , \tag{3}$$

where $s_{11}$ and $s_{21}$ are independent of x. Now integrate (2) from $-\infty$ to $+\infty$, using the first half of (3) as "initial conditions". As $x \to \infty$, we can find $s_{11}$ and $s_{21}$ as functions of $\lambda$. When $\lambda$ is real, this is analogous to a plane wave (amplitude $s_{11}$) coming from $x=+\infty$ that is scattered by the "potential well" D to produce a transmitted (amplitude 1) and a reflected wave (amplitude $s_{21}$). The reflection coefficient is $\rho(\lambda)=s_{21}/s_{11}$. When $\lambda$ is complex (let $\lambda=\lambda_r+i\lambda_i$, $\lambda_r>0$ and $\lambda_i>0$, so that $\mathrm{Im}(\lambda^2)>0$), $\Psi$ represents a wave packet that is trapped in the potential well at discrete "energy levels" $\lambda=\lambda_n$ (n=1,2,...). Discrete eigenvalues satisfy $s_{11}(\lambda_n)=0$ so that $\Psi$ is bounded as $x \to \infty$. We define the normalizing factor associated with $\lambda_n$, $c_n = is_{21}(\lambda_n)/s_{11}'(\lambda_n)$ where $s_{11}'(\lambda_n)$ is the derivative of $s_{11}$ with respect to $\lambda$, evaluated at $\lambda=\lambda_n$. The set $\{\rho(\lambda), \lambda_n, c_n\}$ is called the scattering data.

The time dependence of the scattering data is given by linear equations,

$$\rho(\lambda,t)=\rho(\lambda,0)e^{-4i\lambda^4 t} \ ; \ \lambda_n(t)=\lambda_n(0) \ ; \ c_n(t)=c_n(0)e^{-4i\lambda_n^4 t} , \tag{4}$$

so we can easily advance the scattering data in time; one then solves the so-called Gel'fand-Levitan integral equations to reconstruct b(x,t) at later times. First, define, using the scattering data (hereafter, dependency on t is omitted)

$$F(z) = \sum_k c_k \exp(i\lambda_k^2 z) + \frac{1}{2\pi}\int_{-\infty}^{\infty} \rho(\lambda)\exp(i\lambda^2 z)d\lambda . \tag{5}$$

Next, solve the pair of integral equations

$$L(x,y) - i\int_x^{\infty} K(x,s)F'(s+y)ds = 0 , \tag{6a}$$

$$K(x,y) + F^*(x+y) + \int_x^{\infty} L(x,s)F^*(s+y)ds = 0 . \tag{6b}$$

The solution to the above gives

$$b(x,t) = -2K(x,x)\exp\left[-4i\int_x^{\infty} |K(x',x')|^2 dx'\right] . \tag{7}$$

Note that all the equations used in the IST are linear; although they look more complicated than the original nonlinear equation, there are general techniques for finding their solutions.

To show the correspondence between a discrete eigenvalue and an envelope soliton, let us suppose there is a single discrete eigenvalue at $\lambda$ and $\rho(\lambda)=0$. Let us define $L=L_r+iL_i=\lambda^2$. Then from (5), $F(z)=c\exp(i\lambda^2 z)$, and we find from (6)

$$K(x,y) = \frac{c^* \exp[-iL^*(x+y)]}{(|c|^2 L/4L_i^2)\exp(-4L_i x) - 1} . \tag{8}$$

By using (7) we find

$$b(x,t) = a(\xi)\exp(i\varphi_0 + i\varphi(\xi) + i\Omega t) , \tag{9a}$$

where $\xi=(x-x_0)-v(t-t_0)$, $v=4L_r$, $x_0$, $t_0$, and $\varphi_0$ are real constants, and

$$a^2(\xi) = \frac{8L_i^2}{|L|\cosh(4L_i\xi) - L_r} , \tag{9b}$$

$$\varphi(\xi) = -2L_r\xi + 3\tan^{-1}\left[\frac{L_i}{|L| - L_r}\tanh(2L_i\xi)\right] , \tag{9c}$$

$$\Omega = -4|L|^2 . \tag{9d}$$

This is the "two-parameter" envelope soliton, so named because it has two free parameters, $\lambda_r$ and $\lambda_i$. Other DNLS solitons are discussed in Mjølhus and Wyller (1986).

## Numerical Example

To illustrate the use of the IST, we numerically integrated the DNLS with periodic boundary conditions in time using the Fourier spectrum method, and also computed the evolution of the scattering data using the initial magnetic field profile as input. Our results are summarized in Figure 1. The panels in the left-most columns of Figure 1(a)-(c) show the time evolution of the transverse magnetic field, $b_y$, $b_z$, and the envelope plotted versus x. The initial wave-packet profile in Figure 1(a) starts to split into three solitary wave packets (panel (b)) at time=5; at time=10 they have separated further, since each soliton has a different speed. The Fourier power spectrum of the magnetic field is plotted versus log|k|, where k is the wave number; the left- and right-hand sides correspond to k<0 (LHP) and k>0 (RHP), respectively. The wave is initially predominantly LHP, but later, wave-wave coupling transfers some power to RHP modes. One cannot conclude much from the Fourier analysis of this nonlinear system: comparison of the Fourier spectra at

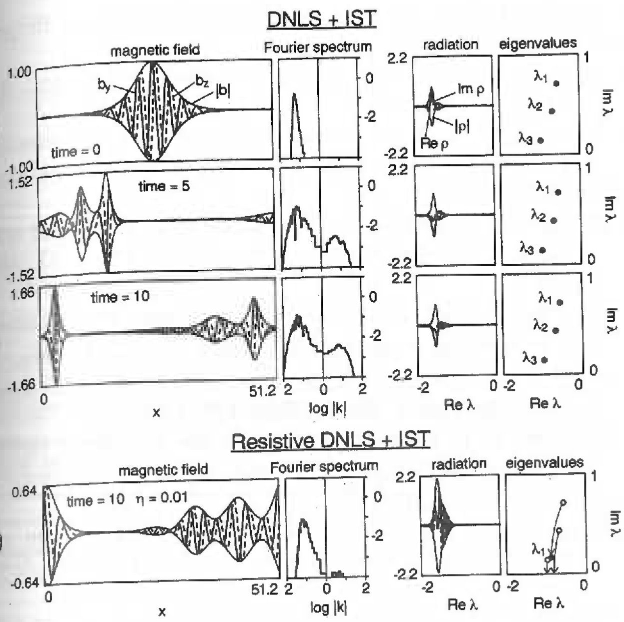


Fig. 1. Evolution of Alfvén waves in the DNLS system and the scattering data computed by inverse scattering transform (IST) associated with the DNLS (equations (1) and (12), with $\alpha=\delta=1$). Shown are, from left to right: time evolution of the transverse magnetic field and the envelope plotted versus the main axis, x; the Fourier power spectrum; the "radiation" part of the scattering data plotted versus $\lambda$; and the discrete eigenvalues in the phase space $\mathrm{Re}(\lambda)$-$\mathrm{Im}(\lambda)$.

time=0, 5, and 10 would not reveal that the DNLS has an infinite number of invariants, for example.

Below we describe how to calculate the "radiation" $\rho(\lambda)$ and the discrete eigenvalues, $\lambda_n$, from magnetic field data. Although our simulation has periodic boundary conditions, in the case of a single wave-packet whose envelope approaches zero at both ends, we may use the IST for "vanishing boundary conditions" provided the packet remains isolated in the simulation system.

Let us define two points, $x_1$ and $x_2$, at which $|b|\sim 0$, such that the wave-packet is contained between them. For our initial profile, we may choose $x_1=0$ and $x_2=51.2$; then we calculate $\rho(\lambda)$, taking $\lambda$(=real) as a parameter. First, we define

$$\Psi(x_1) = \begin{bmatrix} e^{-i\lambda^2 x_1} \\ 0 \end{bmatrix}, \tag{10}$$

and then numerically integrate $\Psi$ from $x_1$ to $x_2$, using equation (2), and find $\Psi$ at $x=x_2$,

$$\Psi(x_2) = \begin{bmatrix} s_{11}e^{-i\lambda^2 x_2} \\ s_{21}e^{i\lambda^2 x_2} \end{bmatrix}, \tag{11}$$

and $\rho(\lambda)=s_{21}/s_{11}$.

The eigenvalue, $\lambda_n$, is obtained in a similar way. We again define $\Psi(x_1)$ by (10), this time with complex $\lambda$. Numerically integrating equation (2), we find $\Psi(x_2)$, written in the form of (11). This gives $s_{11}(\lambda)$ and $s_{21}(\lambda)$ as complex functions of $\lambda$. We then obtain $\lambda_n$, the roots of $s_{11}(\lambda)=0$, using, for example, Muller's method (Press *et al.*, 1986).

The two columns on the rhs of Figure 1 show $\rho(\lambda)$ and $\lambda_n$, computed from magnetic field data at various time steps. The envelope of $\rho(\lambda)$ along with its real and imaginary parts are plotted versus $\lambda$(=real); discrete eigenvalues are shown as closed circles in $\mathrm{Re}(\lambda)$-$\mathrm{Im}(\lambda)$ space. There are 3 discrete eigenvalues and the initial wave evolves into 3 envelope solitons. Despite the drastic change in field profile, the eigenvalues and the radiation envelope remain unchanged.

Should the waves not obey the DNLS, the scattering data will not be invariant. Figure 1(d) shows the evolution of the wave and the scattering data when resistive damping is added to the DNLS,

$$\frac{\partial b}{\partial t} + \alpha\frac{\partial}{\partial x}(|b|^2 b) + i\delta\frac{\partial^2 b}{\partial x^2} = \eta\frac{\partial^2 b}{\partial x^2}, \tag{12}$$

where $\eta$ is the resistivity. We solved (12) for the initial profile in Figure 1(a) with $\eta=0.01$. Figure 1(d) shows the profile, the Fourier power spectrum, and the scattering data at time=10. Clearly, neither the radiation nor the eigenvalues were invariants: the eigenvalues gradually approached the real axis (their locations at t=0 are shown as open circles), while the radiation amplitude increased. However, the behavior is compactly described as decaying solitons.

## Discussion

By applying the DNLS-IST to intervals of data for which the DNLS approximation is roughly valid, we would be able to study:

- Past history of the waves. The scattering data reveals the origin and past history of the waves. For example, we can ask whether a sequence of wave packets shared a common origin in a finite amplitude monochromatic wave, or whether they originated in different locations.
- Future evolution of the waves. We could compare the DNLS prediction from one data set with that obtained later on a nearby spacecraft.
- Soliton statistics. Since soliton properties (speed, amplitude, etc) remain unchanged in interaction with other solitons, the statistical distribution of solitons obtained from solar wind data has meaning and could be compared with that found from numerical simulations.

Even if the DNLS is not strictly valid, the deviation in real data from the DNLS prediction might illuminate what physical processes modify the DNLS.

To develop the IST for data analysis will require new kinds of investigations, first at the applied mathematics and physics level, and subsequently the computational level. More study of the IST in 2 and 3 dimensions is needed; the DNLS-IST should be evaluated in strongly nonlinear systems, or ones involving wave-particle interactions; and ISTs based upon other integrable equations should be explored. Thus, the IST may not become a practical tool for spacecraft data analysis in the very near future. However, the rapid advances in workstation capability suggests that people will soon be willing to spend what

seem today major computational and analytical resources on a variety of sophisticated data- and physics-adapted transforms. Eventually, such computing power will be put on spacecraft, to minimize the costs of data transport. From this perspective, it seems important to begin exploring advanced transforms now. The ultimate goal is to search data interactively for its representation in terms of all the self-organized structures compatible with the known or hypothesized physics of the system under study—not only solitons, but also such things as shocks and vortices.

*Acknowledgments.* We thank B. Buti, F. V. Coroniti, Y. H. Ichikawa, M. B. Kennel, E. Mjølhus, M. Nambu, and C. C. Wu for useful discussions. This research was supported by NASA NAGw-1624.

## References

Burlaga, L. F., Heliospheric magnetic fields and plasmas, *Rev. Geophys., 21*, 363-375, 1983.

Greenstadt, E. W. *et al.*, Correlated magnetic field and plasma observations of the earth's bow shock, *J. Geophys. Res., 73*, 51, 1968.

Hoppe, M. M. *et al.*, Upstream hydromagnetic waves and their association with backstreaming ion populations: ISEE 1 and 2 observations, *J. Geophys. Res., 86*, 4471, 1981.

Hoppe, M. M., *et al.*, Characteristics of the ULF waves associated with upstream ion beams, *J. Geophys.Res.*, 87, 643, 1982.

Kaup, D. J., and A. Newell, An exact solution for a derivative nonlinear Schrödinger equation, *J. Math. Phys., 19*, 798-801, 1978.

Kawata, T., and H. Inoue, Inverse scattering method for the nonlinear evolution equations under nonvanishing conditions, *J. Phys. Soc. Jpn., 44*, 1968-1729, 1978.

Kawata, T. *et al.*, Inverse method for the mixed nonlinear Schrödinger equation and soliton solutions, *J. Phys. Soc. Jpn., 48*, 1371-1379, 1980.

Kennel, C. F. *et al.*, Plasma and energetic particle structure upstream of a quasi-parallel interplanetary shock, *J. Geophys. Res., 89*, 5419, 1984a.

Kennel, C. F. *et al.*, Structure of the November 12, 1978, quasi-parallel interplanetary shock, *J. Geophys. Res., 89*, 5436, 1984b.

Kennel, C. F. *et al.*, Nonlinear, dispersive, elliptically polarized Alfvén waves, *Phys. Fluids, 31*, 1949, 1988.

Mio, K. *et al.*, Modified nonlinear Schrödinger equation for Alfvén waves propagating along the magnetic field in cold plasmas, *J. Phys. Soc. Jpn., 41*, 265, 1976.

Mjølhus, E., Rep. 48, Dept. of Appl. Math., Univ. of Bergen, Norway, 1974.

Mjølhus, E. and J. Wyller, Alfvén solitons, *Phys. Scr., 33*, 442-451, 1986.

Press, W. H. *et al., Numerical Recipes, The Art of Scientific Computing, Cambridge University Press, Cambridge*, pp.262, 1986.

Prikarpatskii, A., Almost periodic solutions of a modified nonlinear Schrödinger equation, *Theor. Math. Phys., 47*, 487, 1981.

Rogister, Parallel propagation of nonlinear low-frequency waves in high-β plasma, *Phys. Fluids, 14*, 2733, 1971.

Scarf, F. L. *et al.*, Plasma wave observations at comet Giacobini-Zinner, *Science, 232*, 377, 1986.

Sentman, D. D. *et al.*, Instabilities of low frequency, parallel propagating electromagnetic waves in the earth's foreshock region, *J. Geophys. Res., 86*, 7487-7497, 1981.

Smith, C. W. *et al.*, Turbulence analysis of the Jovian upstream "wave" phenomenon, *J. Geophys. Res., 88*, 5581, 1983; correction, *J. Geophys. Res., 89*, 9159, 1984.

Spangler, S. R., and J. P. Sheerin, Properties of Alfvén solitons in a finite-β plasma, J. Plasma Phys., 27, 193, 1982; Corrigendum, *J. Plasma Phys., 32*, 347, 1985.

Tsurutani, B. T., and E. J. Smith, Strong hydromagnetic turbulence associated with comet Giacobini-Zinner, *Geophys. Res. Lett., 13*, 259, 1986a.

Tsurutani, B. T., and E. J. Smith, Hydromagnetic waves and instabilities associated with cometary ion pickup: Ice observations, *Geophys. Res. Lett., 13*, 263, 1986b.

Tsurutani, B. T. *et al.*, Highly nonlinear magnetic pulses at comet Giacobini-Zinner, *Geophys. Res. Lett., 17*, 757, 1990a.

Tsurutani, B. T. *et al.*, Discrete phase changes within nonlinear steepened magnetosonic waves: comet Giacobini-Zinner, *Geophys. Res. Lett., 17*, 1817, 1990b.

T. Hàda, Department of Physics, College of General Education, Kyushu University, Ropponmatsu, Chuoku, Fukuoka 810 Japan.

R. L. Hamilton, Program in Applied Mathematics, University of Arizona, Tucson, AZ 85721.

C. F. Kennel, Department of Physics, University of California at Los Angeles, Los Angeles, CA 90024.

(Received: August 11, 1992 ;
revised: December 02, 1992 ;
accepted: December 16, 1992.)